

RESEARCH PAPER



Combined α -programmed death-1 monoclonal antibody blockade and fractionated radiation therapy reduces tumor growth in mouse EL4 lymphoma

Xiuyun Lin^{a,b}, Tao Zeng^c, Jiani Xiong^a, Qiong Zhang^a, Pan Jiang^a, Xiufeng Li^c, Shuchun Lin^{a,b}, Qianqian Xu^c, Huanjiao Weng^c, Haichun Lai^{a,b}, Huichun Gong^c, Jinxiang Lin^c, Niangmei Cheng^a, Xinling Tian^c, Yunlu Xu^a, Shubin Fang^a, Rong Jin^c, Zhiwei Chen^d, Jianbo Yang^e, Luke Morton^e, Bevan Yueh^e, and Jizhen Lin^{a,b,e}

^aInstitute of Immunotherapy, Fujian Medical University, Fuzhou, China; ^bFujian Medical University Union Hospital, Fuzhou, China; ^cImmunotherapy Research and Development, CreMab Biopharma, Inc, Fuzhou, China; ^dFuzhou Center for Disease Control and Prevention, Fuzhou, China; ^eDepartment of Otolaryngology, Medical School, University of Minnesota, Minneapolis, Minnesota, USA

ABSTRACT

The programmed death (PD) pathway is frequently present in the tumor microenvironment (TME) and suppresses tumor immunity by inhibiting the activity of tumor-infiltrating lymphocytes (TILs), particularly, CD8⁺ lymphocytes. PD immunotherapy involves stimulation of the immune response in the region surrounding the tumor but is insufficient to prevent tumor progression. Therefore, in this study, we examined the effects of combined PD immunotherapy with fractionated radiotherapy (RT) on antitumor immunity and tumor growth in lymphoma.

The immune cell profiles of the TME, blood, and secondary lymphoid organs were determined 7 days after treatment. Four combination therapies were compared. The synergistic effects of α PD-1 mAb and fractionated RT on increased CD8⁺ lymphocytes in the TME, blood, and secondary lymphoid organs led to substantial tumor regression in mouse EL4 lymphoma, both locally and systemically. Fractionated RT for 4 days followed by α PD-1 mAb therapy was significantly superior to other schemes in terms of overall survival rates and curative rates in xenograft model mice. Our data indicated that substantial immune responses occurred following combination therapy with fractionated RT and α PD-1 mAb immunotherapy. Our findings provide important insights into the use of RT plus α PD-1 mAb as an efficacious combinatorial therapy.

ARTICLE HISTORY

Received 8 August 2018
Revised 3 November 2018
Accepted 15 November 2018

KEYWORDS

fractionated radiotherapy; programmed death-1; programmed death ligand-1; antitumor immunity; scheme

Introduction

Approximately 50–60% of patients with malignancies undergo traditional therapies.¹ Fractionated radiotherapy (RT) is often used because it has fewer toxic effects in healthy cells than single high doses of RT, and emerging evidence demonstrates that fractionated RT is more immunogenic.^{2,3} Fractionated RT has also been shown to cause tumor cell apoptosis and necrosis through DNA damage, resulting in immunogenic cell death (ICD).⁴ ICD of cancer cells is mediated by damage-associated molecular patterns (DAMP),⁵ which facilitate the activation and migration of antigen-presenting cells (APCs) and thereby modulate the maturation and accumulation of cytotoxic T lymphocytes (CTLs).^{6,7} However, disease relapse still occurs frequently due to a variety of resistance mechanisms related to fractionated RT monotherapy.

Programmed death (PD) protein is highly expressed in the tumor microenvironment (TME) and is related to immunosuppression of antitumor immunity in some patients, particularly those with immunogenic tumors.⁸ In the presence of chronic inflammation, inflammatory cytokines and chemokines frequently induce PD-ligand 1 (PD-L1) protein expression.⁹ PD-L1 interacts with its receptor PD-1, which is highly expressed on activated lymphocytes, leading to anergy,

exhaustion, and apoptosis of tumor-infiltrating lymphocytes (TILs).^{10–12} Furthermore, tumors with extensive PD-L1 expression and lymphocyte infiltration have been shown to respond well to α PD-1/PD-L1 monoclonal antibody (mAb) therapy.^{13–15} Clinical trials and murine tumor models have shown promising antitumor effects in response to blockade of the PD pathway.^{16–19} However, only approximately 20% of patients with malignancies respond to PD pathway blockade.^{20,21} Therefore, it is necessary to combine PD immunotherapy with fractionated RT to increase antitumor immunity through exposure to tumor antigens.

The abscopal effect is a clinically rare phenomenon that occurs after irradiation treatment.^{22,23} R.H. Mole first coined the term “abscopal” in 1953 to describe that tumors would shrink not only in the irradiated lesion, but also in out-of-field lesions.²⁴ Thus, PD immunotherapy in combination with fractionated RT may significantly increase the abscopal effect. Indeed, PD immunotherapy has been shown to rescue the activity of TILs, whereas fractionated RT increases the exposure of tumor antigens; these effects could allow antitumor immunity in the TME to be persistent and durable.

In this study, we examined the effects of fractionated RT, which may alter the activity of TILs in the TME,^{25,26} on the

expression of PD-L1. Furthermore, we assessed immune cell subsets across organs and tissues, locally and systemically. Our results provide important insights into the effects of fractionated RT in combination with α PD-1 mAb immunotherapy on tumor growth and progression.

Results

Abscopal effects of combination therapy in the EL4 lymphoma model

To understand how fractionated RT altered T-cell surface molecules, EL4 cells were irradiated with increasing doses of fractionated RT (0 Gy, 8 Gy \times 2, 15 Gy \times 2, 25 Gy \times 2, once a day) *in vitro*, and the expression of PD-L1 following fractionated RT was assessed. PD-L1 expression was elevated after exposure to fractionated RT, even though EL4 cells barely expressed PD-L1 at the baseline *in vitro* (Figure 1(a,b)). To address whether fractionated RT in combination with α PD-1 mAb triggered systemic antitumor immune responses, mice were treated with control immunoglobulin G (IgG), α PD-1 mAb alone, RT plus control IgG, and RT plus α PD-1 mAb. Two fractionated RT doses of 8 Gy were delivered to a single tumor (primary tumor), and the contralateral tumor was set outside the radiation field (Figure 1(c)). Our data demonstrated that α PD-1 mAb slightly suppressed primary tumor progression compared with that in time-matched, control IgG mice ($P < 0.001$). Fractionated RT as a single modality caused significant growth delay in the primary tumor; however, on day 19, the tumor showed progressive growth. Fractionated RT plus α PD-1 mAb more effectively inhibited tumor growth than did monotherapy (Figure 1(d)), with complete regression observed in some mice.

Interestingly, combination therapy mediated synergetic abscopal responses in nonirradiated tumor lesions. α PD-1 mAb alone halted the growth of contralateral tumors whose sizes remained stable. Fractionated RT resulted in transient tumor control followed by regrowth in most mice. Treatment with a combination of fractionated RT and α PD-1 mAb significantly controlled contralateral tumor growth (Figure 1(e)). The data indicated that fractionated RT alone was inadequate to generate durable and systemic anticancer immunity. In contrast, treatment with RT plus α PD-1 mAb triggered adaptive immune responses, leading to the regression of both irradiated and out-of-field tumors.

Long-term surviving (LTS) mice after first tumor challenge (60 days after first challenge), but not naïve mice, were resistant to a subsequent rechallenge with EL4 cells (Figure 1(f)), demonstrating that the combination of α PD-1 mAb and fractionated RT generated systemic antitumor immunity in mice.

Combination therapy remodels the TME in irradiated and distant tumor lesions

We analyzed changes in the immune cell profiles of the TME 7 days after treatment, by immunohistochemistry (IHC). Analysis of the patterns of tumor-infiltrating effector T cells showed that the proportions of CD3⁺, CD8⁺ and CD4⁺ TILs were increased in fractionated RT- and α PD-1 mAb-treated

mice when compared with control IgG-treated mice. The frequencies of CD3⁺, CD8⁺ and CD4⁺ TILs in the combination therapy group were higher than those in the RT- or α PD-1 mAb monotherapy groups for both irradiated and out-of-field tumors (Figure 2(a,b)), and Figure 3). However, the number of FOXP3⁺ T regulatory cells (Tregs) was reduced in mice receiving combination therapy compared with that in mice receiving monotherapies (Figure 2(a,b)), and Figure 3). These changes in effector and immunosuppressive cells gave rise to significantly elevated ratios of both effector CD4⁺ and CD8⁺ T cells to Tregs in TILs of mice receiving combination therapy (Figure 2(c,d)). In addition, we assessed the numbers of NK cells and macrophages in the TME. The emergence of M1 macrophages (iNOS⁺) and NK cells was apparent in the combination therapy group compared with the control IgG groups for both irradiated and out-of-field tumors. However, combination therapy slightly increased the density of M2 macrophages (ARG1⁺) compared to the monotherapy or control IgG group. Consequently, combination therapy significantly increased the ratio of M1 to M2 macrophages in the TME (Figure S1).

In a pilot study, we found that fractionated RT could lead to expression of PD-L1 *in vitro*. Therefore, we next examined whether PD-L1 expression could be induced *in vivo*. We compared PD-L1 expression between experimental and control mice on day 7 after the last dose of fractionated RT (Figure 2(e,f)). The results showed that tumors from mice that had received combination therapy exhibited more intense staining for PD-L1 than those from control mice. However, this increase was more evident in fractionated RT-treated mice. In addition, we assessed changes in PD-1 expression and found increased expression of PD-1 in the fractionated RT group, but reduced expression in the α PD-1 mAb monotherapy and combination therapy groups compared with those in control mice (Figure S2A, 2B). The proportions of MHC class I and class II proteins in the combination therapy group were higher than those in the monotherapy or control IgG groups for both irradiated and contralateral lesions (Figure S3).

Lymphocyte activation and proliferation are observed in secondary lymphoid organs

Next, we assessed the immune cell profiles of the spleen; although immune cells of the spleen often do not directly contact the tumor, they are often analyzed when assessing the mechanisms mediating therapeutic effects in cancer. Several clusters of lymphocytes increased in frequency on day 7 after therapy. The emergence of CD8⁺ and CD4⁺ T cells was apparent in the combination therapy group compared with the monotherapy groups (Figure 4(a,b)). The percentage of myeloid-derived suppressor cells (MDSCs, CD11b⁺Gr1⁺) decreased in the combination therapy group (Figure 4(b)). Moreover, the ratios of CD4⁺ and CD8⁺ T cells to MDSCs were increased in the combination therapy group (Figure 4(c)). Alterations in other subsets were observed, including macrophages (CD11b⁺ F4/80⁺) and dendritic cells (DCs, CD11c⁺). The numbers of macrophages and DCs, as APCs, were enhanced in the combination therapy group (Figure 4(d)). Additionally, CD45⁺ cells showed enhanced Ki-

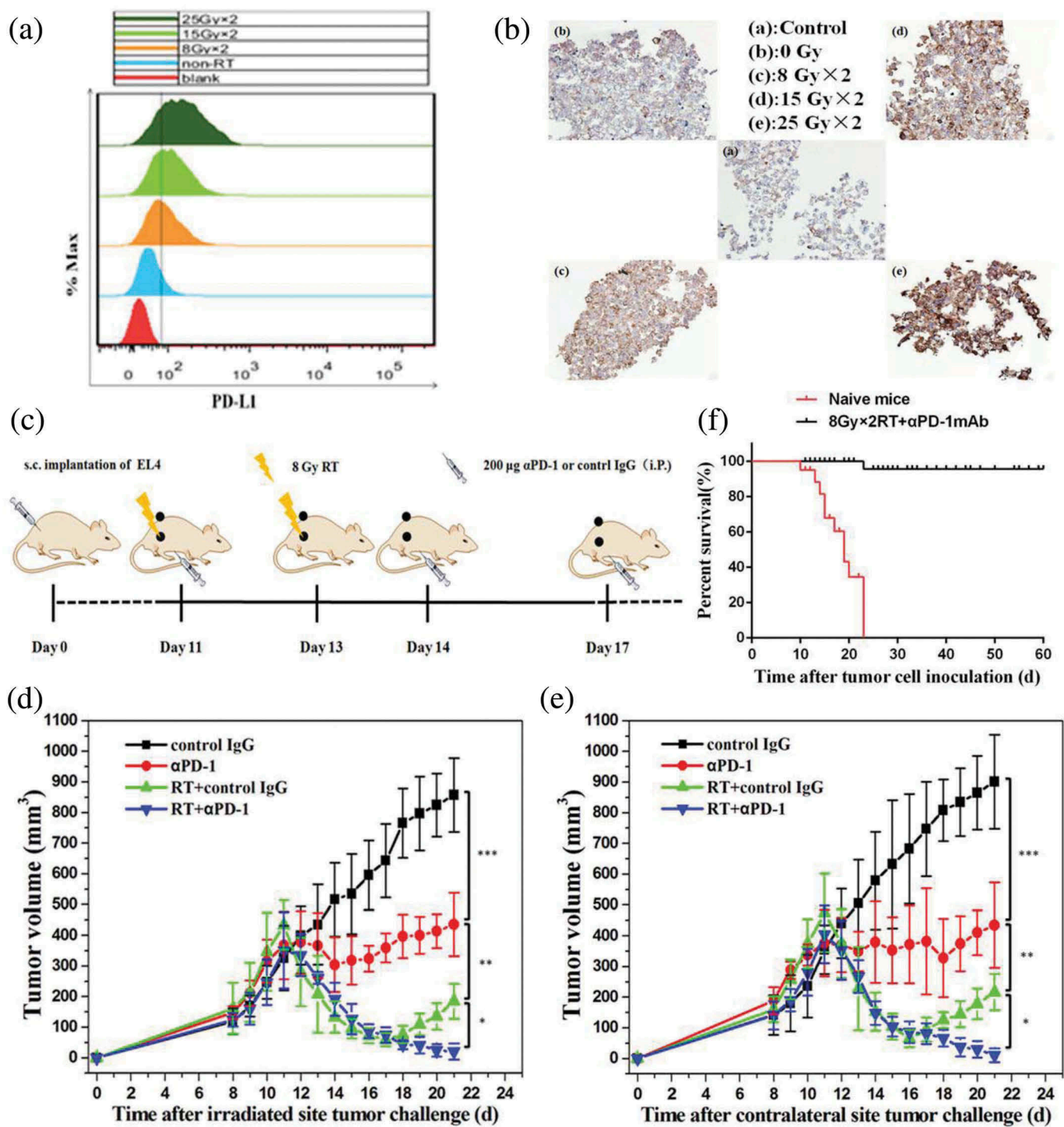


Figure 1. Fractionated RT and αPD-1 mAb work synergistically to enhance therapeutic efficacy against EL4 lymphoma.

EL4 lymphoma cells were irradiated with increasing doses of fractionated RT (0 Gy, 8 Gy × 2, 15 Gy × 2, 25 Gy × 2, once a day). Representative flow cytometry (a) and immunostaining images (b) of PD-L1 expression in EL4 cells 24 h after the last dose of radiation. (c) Scheme of tumor engraftment and combination therapy; only the primary tumors received RT as indicated. (d) and (e) Subcutaneous tumor volume measurements (means ± SDs) of irradiated tumors (d) and contralateral tumors (e) with the indicated regimens. Data are shown as means ± SDs. Experimental groups contained at least five mice and are representative of at least three independent experiments. (f) Overall survival of tumor-free mice receiving combination therapy. The mice were rechallenged at a distant site 60 days after the first challenge. Experimental groups contained at least five mice, and data are representative of at least three independent experiments. **P* < 0.05; ***P* < 0.01; ****P* < 0.001. RT, radiotherapy.

67 expression as a proliferation marker (Figure 4(e)). Proliferation in the spleen was consistent with the TME.

We also analyzed the draining lymph nodes (DLNs) of primary tumors, in which T-cell priming was stimulated as

part of the systemic response. Changes in T-cell subsets coincided with those in the spleen. Combination therapy resulted in significant expansion of CD3⁺ CD8⁺ and CD3⁺ CD4⁺ T cells (Figure 4(f)).

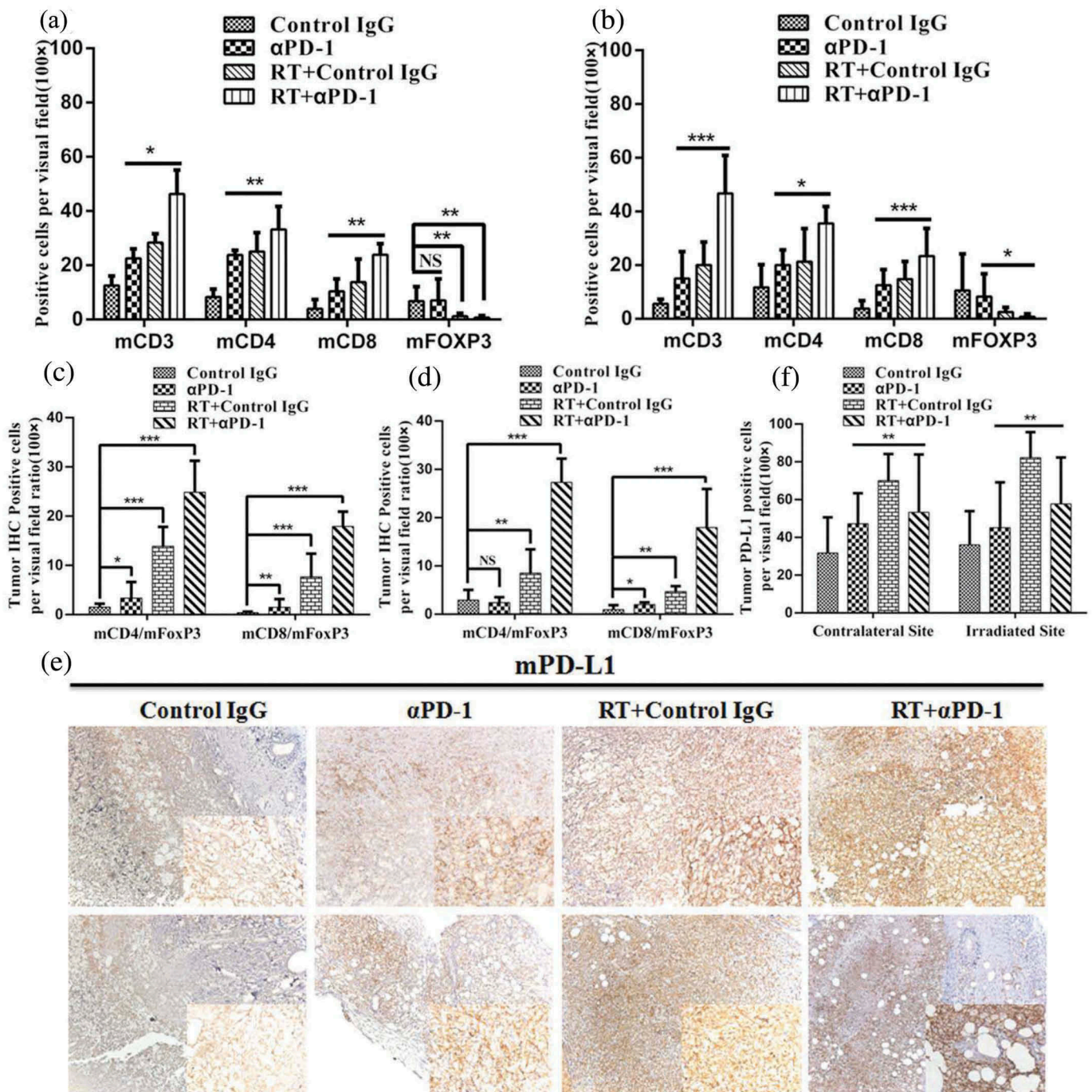


Figure 2. Combination therapy reverses the highly immunosuppressive milieu to an immunostimulatory milieu by increasing effector T cells and decreasing Tregs. Animals were treated according to the scheme described in Figure 1(c). Tumors were excised 7 days after treatment, and TILs were analyzed with IHC. (a) and (b) Positive cells per visual field of tumor-infiltrating CD3⁺ T, CD4⁺ T, CD8⁺ T, and FOXP3⁺ T cells in irradiated (a) and contralateral (b) lesions. (c) and (d) Ratios of CD8⁺ and CD4⁺ T cells to FOXP3⁺ T cells in irradiated (c) and contralateral (d) lesions. (e) Representative PD-L1 expression in tumors in nonirradiated animals (upper row) and irradiated animals (lower row). (f) Positive cells per visual field of PD-L1 expression in tumor tissues. Data represents cumulative results from 3 independent experiments with 5 mice/group. **P* < 0.05; ***P* < 0.01; ****P* < 0.001. RT, radiotherapy.

Systemic immune responses occur upon combination therapy

To investigate whether the immune responses were systemic, changes in T cells in the peripheral blood were analyzed by flow cytometry. Similar changes were observed in CD3⁺ CD8⁺ T cells, CD3⁺ CD4⁺ T cells, and MDSCs (Figure 5(a,b)). The fractions of CD4⁺ and CD8⁺ T-cell subsets were increased, and populations of circulating monocytes fluctuated, with MDSCs decreasing in frequency. Similarly, the ratios of

CD4⁺ and CD8⁺ T cells to MDSCs were elevated in the combination therapy group (Figure 5(c)).

Combination therapy enhances tumor antigen-specific memory T cells

To assess the effects of either monotherapy or combination therapy on the phenotypes of expanding T-cell subsets,

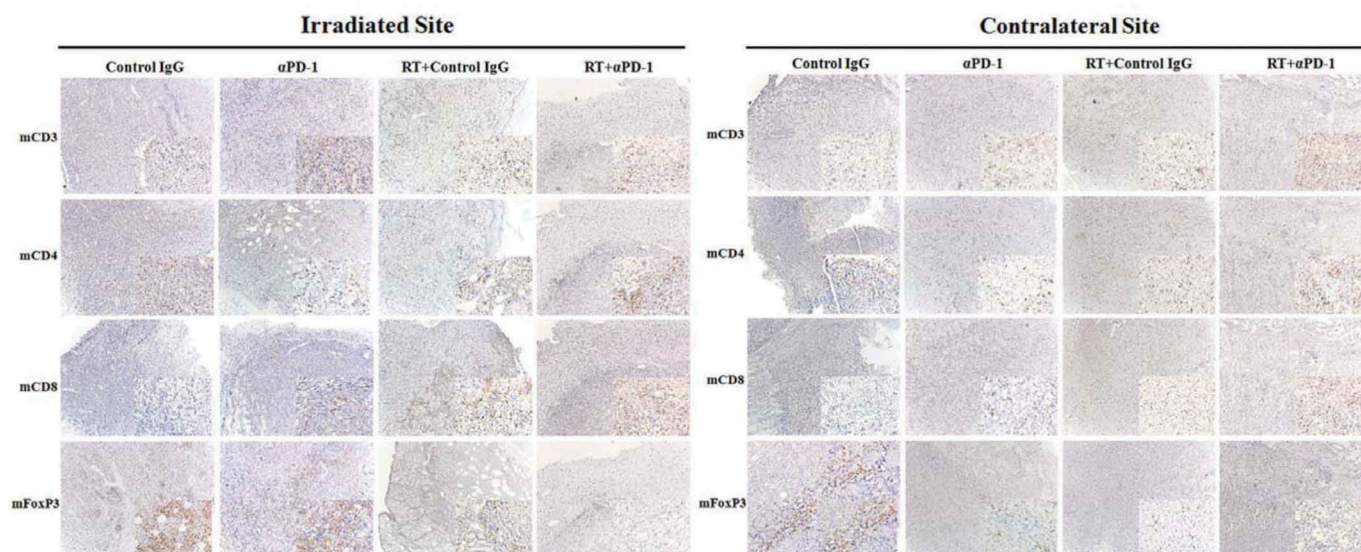


Figure 3. IHC staining of tumor tissues with CD3, CD4, CD8, and FOXP3.

Tumors were excised 7 days after treatment and analyzed with IHC. Representative immunostaining images of CD3⁺ T, CD4⁺ T, CD8⁺ T, and FOXP3⁺ cells in irradiated (left) and contralateral (right) tumors are presented.

CD62L⁺ CD44⁻ cells were defined as native T cells, CD44⁺ CD62L⁻ cells were defined as effector memory cells, and CD44⁺ CD62L⁺ cells were defined as central memory cells. Notably, fractionated RT plus αPD-1 mAb significantly increased the proportions of effector and central memory cells, whereas it decreased the relative percentage of naive cells in the DLNs (Figure 6(a,b)). Interestingly, changes in memory cells in the spleen paralleled those in the DLNs (Figure 6(c)).

Combination therapy stimulates the antigen-specific CD8⁺ t-cell response

Next, we assessed the CD8⁺ T-cell subsets of splenocytes in response to EL4 cells. The splenocytes in the three treatment groups showed significantly increased numbers and dose-dependent CD8⁺ T-cell activity in response to target cells at E/T ratios of 10:1, 20:1, and 40:1 compared with the control group (Figure 7(a)). The cytotoxic activities in the combination therapy group were significantly higher than those in the corresponding control or monotherapy groups ($P < 0.001$ at every ratio, $n = 5$).

We then evaluated the antigen-specific immune response in treated mice. We harvested serum from treated mice and analyzed serum levels of IFN-γ and IL-2 using ELISAs. As shown in Figure 7(b), sera from mice in the combination therapy group contained significantly higher levels of IFN-γ and IL-2 than those of mice in the control or monotherapy groups ($P < 0.001$).

A reasonable regimen of apd-1 mab therapy and RT is required for the induction of an effective systemic immune response

To determine the optimal schedule for combined αPD-1 mAb and fractionated RT that can induce specific and durable antitumor immune responses, we designed four

combination therapy schemes as follows: mice harboring EL4-derived tumors received two fractions of 8 Gy accompanied by application of αPD-1 mAb beginning on day 1 of the fractionated RT cycle (schedule A), on day 3 of the cycle (i.e., on the day of the second fractionated RT; schedule B), 4 days before starting fractionated RT (schedule C), or 4 days after completion of the fractionated RT cycle (schedule D; Figure 8(a)). The data demonstrated that the effects of controlling tumor size in schedules A and D were similar at irradiated sites and out-of-field lesions (Figure 8(b)). Nevertheless, αPD-1 mAb given 4 days before starting fractionated RT (schedule C) did not reduce tumor size well compared with schedules A, B, and D. Interestingly, there were clear differences in overall survival rates and complete tumor regression. With regard to survival rates, schedule D was found to be significantly superior to the other schedules (Figure 8(c)). In addition, the curative rates were 33.33%, 50%, 25%, and 71.43% at the irradiated tumor and 16.67%, 40%, 0%, and 57.14% at the contralateral tumor for schedules A, B, C, and D, respectively (Figure 8(d)). We further assessed changes in immune cell profiles in the spleen, DLNs, and blood in mice subjected to schedules A, B, C, and D. There were no significant differences in CD3⁺ CD8⁺ T cells, CD3⁺ CD4⁺ T cells, and macrophages between schedules A and D; however, the ratios of both effector CD4⁺ T cells and CD8⁺ T cells to MDSCs were increased under schedule D (Figures 9, 10, Figure S4 and Figure S5A-5C). The emergence of NK cells was apparent in schedule D. In addition, we assessed changes in Class I and Class II MHC proteins in the four combination therapy groups. There were no significant differences among groups A, B, and D. However, the group C significantly decreased the expression of MHC Class I and Class II proteins compared with the other groups (Figure S5).

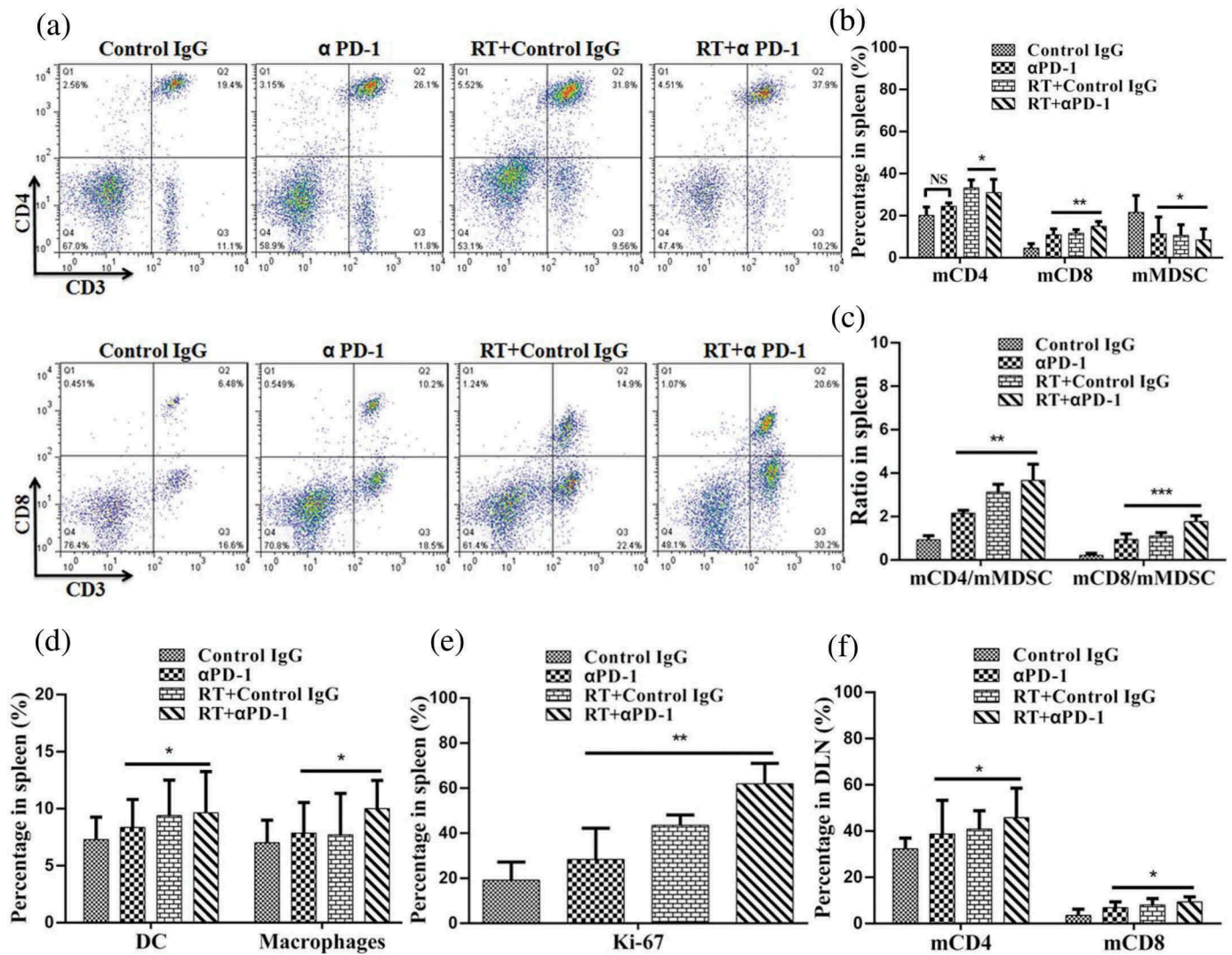


Figure 4. Combination therapy enhances lymphocyte activation and proliferation in secondary lymphoid organs.

(a) Representative flow cytometry plots showing the percentages of CD3⁺, CD4⁺, and CD8⁺ T cells in the spleen. (b) Cumulative results of CD4⁺ T cells, CD8⁺ T cells, and MDSCs (CD11b⁺Gr1⁺) in the spleen. (c) Ratios of CD8⁺ T and CD4⁺ T cells to MDSCs in the spleen. (d) Representative percentage of DCs and macrophages in the spleen. (e) Quantification of Ki-67 expression in CD45⁺ cells in the spleen. (f) Cumulative results of CD4⁺ T cells and CD8⁺ T cells in the DLNs. Representative results from three independent experiments with five mice/group. **P* < 0.05; ***P* < 0.01; ****P* < 0.001. RT, radiotherapy.

In summary, schedule D, which involved αPD-1 mAb administration 4 days after completion of fractionated RT, was found to be the superior schedule.

Discussion

In this study, we demonstrated that fractionated RT increased the expression of PD-L1 in tumor cells *in vitro* and *in vivo*. We observed that combination therapy of fractionated RT and αPD-1 mAb advantageously elicited systemic and local antitumor immunity, with concomitant increases in the percentages of TILs in the local tumor tissue and CD8⁺ T cells in the bloodstream, spleen, and DLN in mice. This combination therapy inhibited the growth of irradiated tumors and out-of-field tumors (abscopal effects). Furthermore, our data revealed that the best combination therapy was fractionated RT for 4 days, followed by αPD-1 mAb immunotherapy.

The synergistic effect of combining immunotherapy with RT has been demonstrated in preclinical models, particularly

in tumors with mutational processes, such as melanoma, head and neck cancer, and colorectal cancer.^{27,28} Malignancies of hematopoietic origin can also be ideal candidates for combination therapy of fractionated RT and αPD-1 mAb. The underlying mechanisms of abscopal effects observed in this study need to be determined in future studies. Moreover, additional studies are needed to determine the diversity of T-cell subsets in the tumor and their specific T-cell receptor.

Interestingly, we observed that combination therapy induced a systemic as well as a local/regional change in antitumor immunity. These changes were involved in the improvement of the immunosuppressive TME by the αPD-1 mAb as evidenced by the abundant TILs in irradiated and out-of-field lesions, especially CD3⁺ CD8⁺ T cells, which kill tumor cells and eliminate tumor lumps in mice. Numerous studies have focused on harnessing CD8⁺ rather than CD4⁺ T cells, because CD8⁺ T cells can specifically kill tumor cells, whereas CD4⁺ T cells cannot. In this study, we demonstrated that both CD8⁺ and CD4⁺ T cells were

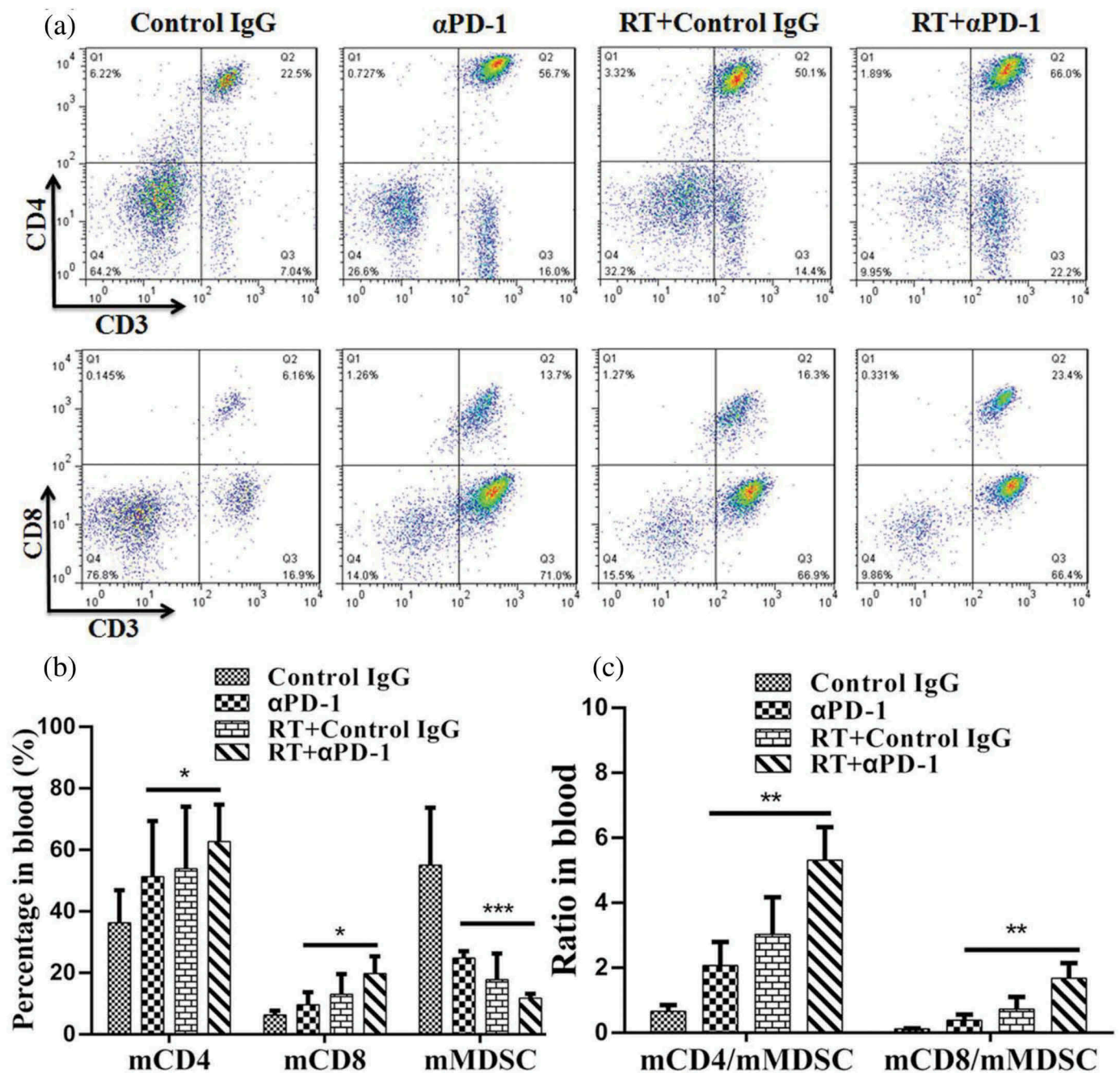


Figure 5. Combination therapy induces increases in both CD4⁺ and CD8⁺ T cells.

(A) Representative flow cytometry plots showing the percentage increases in CD3⁺, CD4⁺ and CD8⁺ T cells in the blood. (B) Cumulative results of CD3⁺, CD4⁺, CD8⁺ T cells, and MDSCs in the blood. (C) Ratios of CD8⁺ and CD4⁺ T cells to MDSCs in the blood. Representative results from 3 independent experiments with 5 mice/group. * $P < 0.05$; ** $P < 0.01$; *** $P < 0.001$. RT, radiotherapy.

equally elevated locally and systemically. CD4⁺ T cells are important in the production of CD8⁺ T cells, especially in systemic immunity. Notably, in this study, CD8⁺ T cells were the major target of α PD-1 mAb immunotherapy. This may indicate that the PD pathway is more prominent in CD8⁺ T cells than in CD4⁺ T cells in the TME, and *vice versa* in the circulation. Interestingly, CD4⁺ CD25⁺ FOXP3⁺ Tregs were dramatically reduced. These results suggested that combination therapy reversed the highly immunosuppressive environment to produce an immunostimulatory milieu by enhancing effector T cells and suppressing Treg populations, which was more permissive for immune-

mediated tumor destruction. This organism-wide analysis of systemic antitumor immunity showed that the peripheral blood and secondary lymphoid organs were more responsive to combination therapy than to monotherapy. Combination therapy stimulated various immune cell populations into a status of activation and propagation, including increases in DCs, macrophages, and T cells. This indicates that innate and adaptive immune cells are crucially involved in the systemic antitumor immune response. In addition, upregulation of MHC class I and class II proteins, which has been associated with antigen presentation by APCs, was observed upon combination therapy.

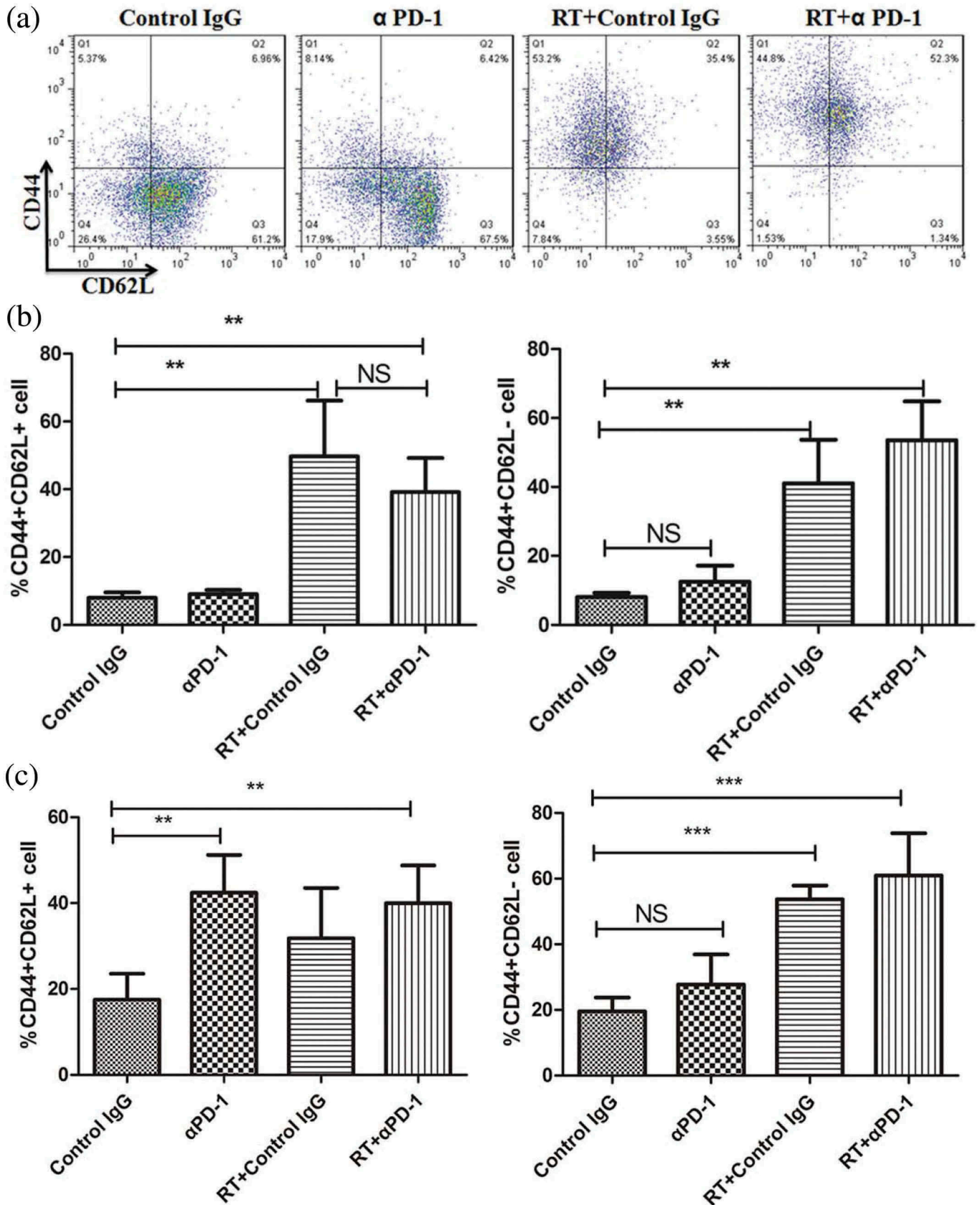


Figure 6. Combination therapy increases tumor antigen-specific memory T cells.

(a) Flow cytometry of putative memory markers in the DLN. (b) and (c) Frequencies of CD44⁺ CD62L⁺ central memory cells (left) and CD44⁺ CD62L⁻ effector/memory cells (right) in the DLN (B) and spleen (c). Data are representative of three independent experiments. ** $P < 0.01$; *** $P < 0.001$. RT, radiotherapy.

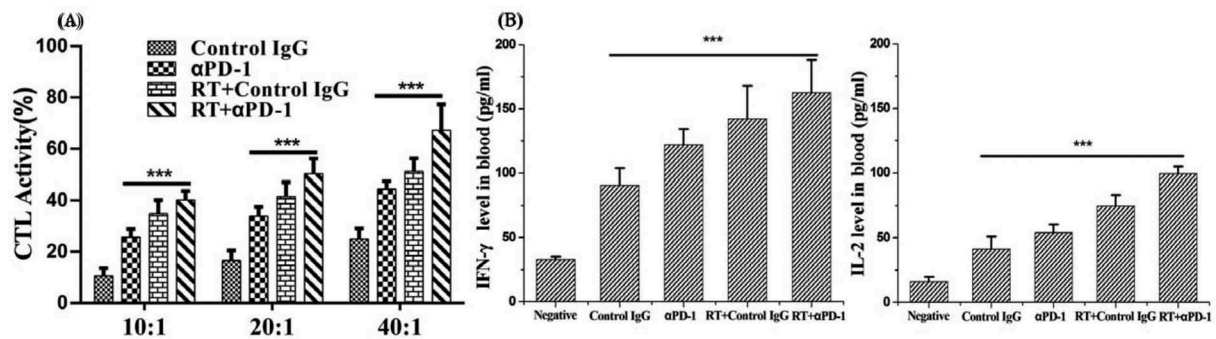


Figure 7. Combination of αPD-1 mAb and RT induced a tumor antigen-specific CTL response in treated mice.

(a) The spleens were collected from the treated mice in each group ($n = 5$) 7 days after treatment, and single-cell suspensions were obtained. The cytotoxic activity of splenocytes at E/T ratios of 10:1, 20:1 and 40:1 were shown. (b) IFN- γ and IL-2 production in the serum from treated mice was determined by ELISA. The results were presented as mean \pm SD. *** $P < 0.001$. RT, radiotherapy.

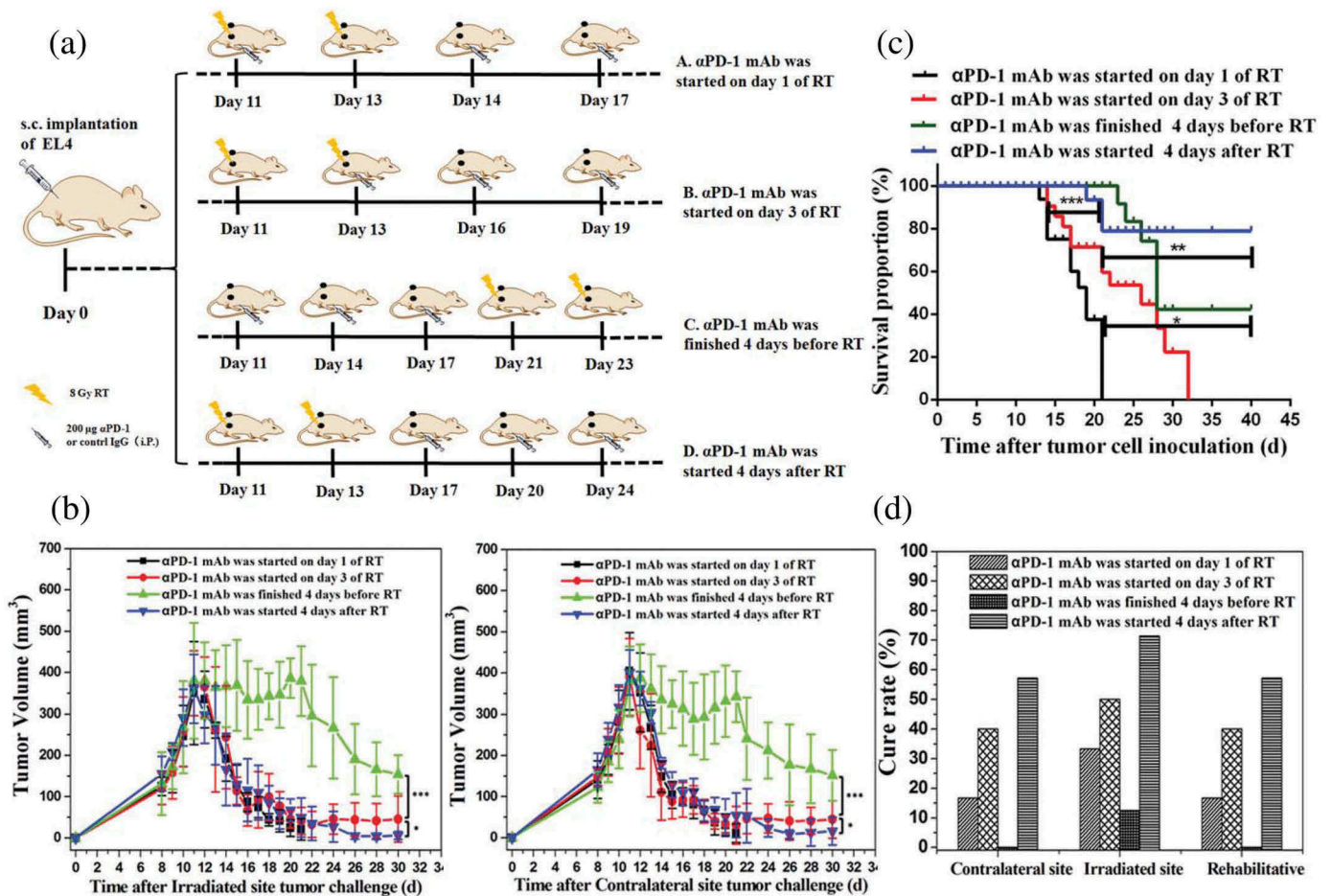


Figure 8. Optimal scheme for combination therapy with αPD-1 mAb and RT in an animal model of EL4 lymphoma.

(a) Treatment scheme for combination therapy. Mice received fractionated RT (as two fractions of 8 Gy RT) alone or in combination with αPD-1 mAb starting on day 1 of the fractionated RT cycle (schedule A), day 3 of the fractionated RT cycle (schedule B), 4 days before starting fractionated RT (schedule C), or 4 days after completion of fractionated RT cycle (schedule D). (b) Average bilateral subcutaneous tumor progression. Data are shown as means \pm SDs. (c) Survival curves. * $P < 0.05$; ** $P < 0.01$; *** $P < 0.001$ (log-rank; Mantel-Cox test). (d) Curative rates. Experimental groups contained at least five mice and are representative of at least three independent experiments.

Furthermore, we assessed the immunological memory phenotypes of the expanding T-cell subsets. Intriguingly, combination therapy significantly improved CD44⁺ CD62L⁻ effector memory cells and CD44⁺ CD62L⁺ central memory cells. These long-term memory cells have the capability to fight back when

tumor cells regrow in the body. This finding prompted us to hypothesize that the combination therapy shifts the TME from an immunosuppressive to an immunostimulatory status and probably induces antitumor immunity memory, which is highly desirable in the clinical setting because these features are a first

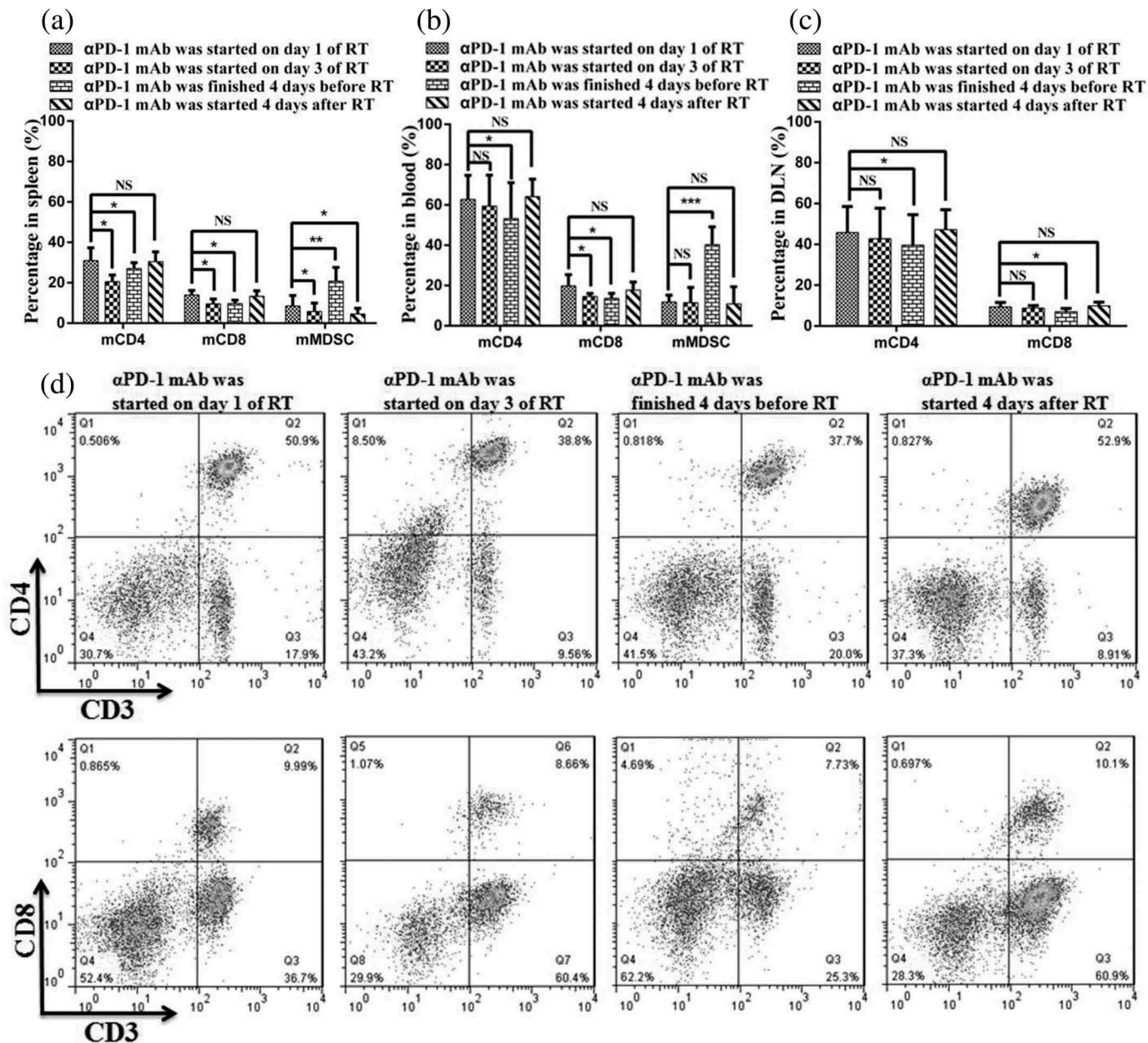


Figure 9. Organism-wide analysis of immune cell responses to combined therapy.

Animals were treated according to the scheme described in Figure 8A. (a) Cumulative results of CD4⁺ T, CD8⁺ T, and MDSCs in the spleen. (b) Cumulative results of CD4⁺ T, CD8⁺ T, and MDSCs in the blood. (c) Cumulative results of CD4⁺ T, and CD8⁺ T in the DLN. (d) Representative flow cytometry plots showing the percentages of CD3⁺, CD4⁺ and CD8⁺ T cells in the DLN. Representative results from 3 independent experiments with 5 mice/group. **P* < 0.05; ***P* < 0.01. RT, radiotherapy.

step in tumor elimination and an indication of regression, respectively. In other words, combination therapy might provide durable anti-tumor immunity.

The synergistic effects of combination therapy on tumor cell elimination in mice were further highlighted by the cytotoxic activity of CD8⁺ T cells in the spleen in EL4 lymphoma-bearing mice when compared with monotherapy. Certain Th1-type cytokines, such as IL-2 and IFN- γ , can enhance the proliferation and differentiation of CD8⁺ T cells. The activated CD8⁺ T cells can accumulate and enhance the adaptive immunity. Therefore, the expression levels of these cytokines are strongly related with the specific cytotoxic activity for antitumor immune responses.^{29,30} Our results showed that combination therapy induced T cells to produce the inflammatory cytokines IL-2

and IFN- γ increase in splenocytes and blood when compared with monotherapy, which may result from combination therapy increasing CD8⁺ T cells in the peripheral T-cell pool.

Few studies have provided preclinical evidence for the optimal sequence of combination therapy. For example, Dovedi and colleagues reported that fractionated RT and α PD-1 mAb immunotherapy should be administered concomitantly in CT26 colon cancer in order to generate a stable systemic antitumor immune response.³¹ Notably, we found that the efficacy of tumor treatment was similar when comparing sequential therapy (α PD-1 mAb immunotherapy 4 days after fractionated RT) with concomitant therapy (α PD-1 mAb immunotherapy 1 day of fractionated RT). However, overall survival rates and complete tumor regression were obviously better upon sequential therapy than after

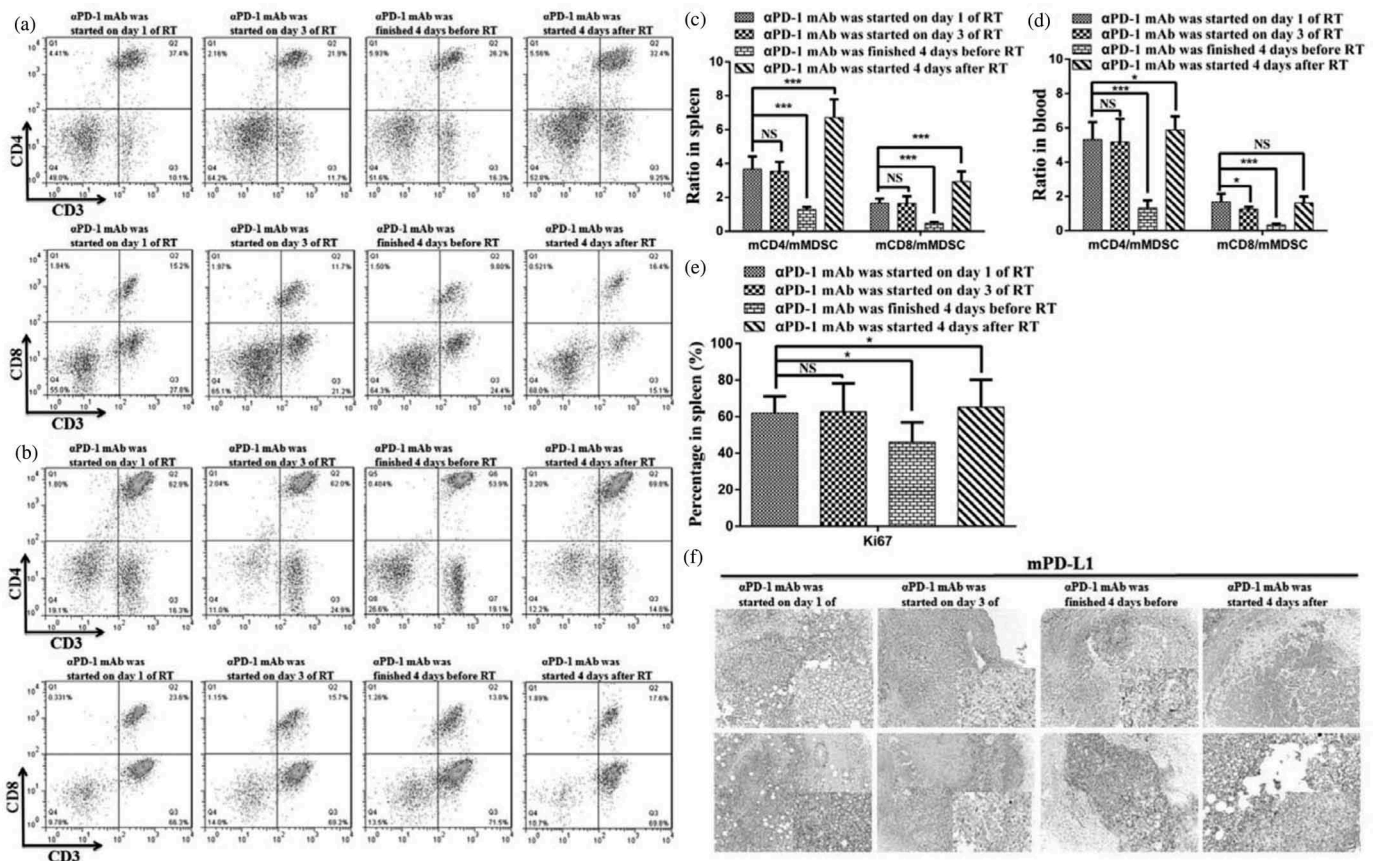


Figure 10. Optimal scheduling of αPD-1 mAb and RT combinatorial therapy is required for effective systemic anti-tumor immune responses.

Animals were treated according to the scheme described in Figure 8A. (a) and (b) Representative flow cytometry plots showing the percentages of CD3⁺, CD4⁺, and CD8⁺ T cells in the spleen (a) and blood (b). (c) and (d) Ratios of CD8⁺ and CD4⁺ T cells to MDSCs in the spleen (c) and blood (d). (e) Quantification of Ki-67 expression in CD45⁺ cells in the spleen. (f) PD-L1 expression in tumors. * $P < 0.05$; ** $P < 0.01$; *** $P < 0.001$. RT, radiotherapy.

concomitant therapy. Heterogeneity in different tumor types, in addition to diversified radiation doses and fractionation, may account for these discrepancies. There are three potential mechanisms that can explain our findings. First, fractionated RT directly killed tumor cells, which could induce necroptosis and apoptosis in tumor cells, thereby releasing tumor antigens. A break of at least 2 days after administration of the last dose of fractionated RT is permitted, giving the immune system time to respond and recover. Application of αPD-1 mAb immunotherapy further promotes immune cell activation, tumor antigen presentation by APCs, DC maturation and migration, TIL formation and expansion, and potent antitumor immune responses. Second, fractionated RT targeting the tumor renders tumor cells fragile and susceptible to the killing of TILs. Elevated PD-L1 levels prepare the system for subsequent αPD-1 mAb immunotherapy. In addition, the time frame of response differs between fractionated RT and αPD-1 mAb immunotherapy. Fractionated RT rapidly kills the tumor cells and releases tumor antigens, which stimulate the formation of tumor-specific lymphocytes. In contrast, αPD-1 mAb immunotherapy improves the activity of these tumor-specific lymphocytes and enhances the continuity and persistence of antitumor immunity; this potent killing of tumor cells by tumor-specific lymphocytes may promote the formation of CD8⁺ memory T cells. Thus, the combination of fractionated RT with αPD-1 mAb therapy is complementary and overcomes the immunotolerance frequently observed in the local TME. This

synergistic action between RT and αPD-1 mAb orchestrates tumor eradication. Therefore, PD immunotherapy reverses T-cell atrophy and dysfunction and improves the TME, whereas RT directly kills the tumor cells, primes TILs, and strengthens tumor immunity.

In summary, our data demonstrated that fractionated RT and αPD-1 mAb combinatorial therapy exhibited strong anti-tumor effects in a mouse EL4 tumor model. Further studies are required to determine the optimal time, dose, and sequence for the combination therapy. Moreover, it is necessary to optimize the combination therapy in the clinical setting to enhance the efficacy of current PD immunotherapy and benefit patients who do not respond to αPD-1 mAb monotherapy.

Materials and methods

Mice

Six- to eight-week-old C57BL/6 mice were purchased from Nanjing WuShi Animal Laboratory and maintained under specific pathogen-free conditions at the animal facility of the Animal Laboratory Center of Fujian Medical University. All animal experiments were performed in accordance with National Institutes of Health guidelines and were approved by the Institutional Animal Care and Use Committee of Fujian Medical University.

Cell line and reagents

EL4 lymphoma cells were purchased from the American Type Culture Collection (Manassas, VA, USA). The cells were routinely screened for the absence of mycoplasma contamination using a mycoplasma detection kit. α PD-1 mAb (clone G4, a hamster IgG1 against mouse PD-1) was used as a blocking mAb for the PD pathway. The α PD-1 mAb was produced and purified as previously described.³² The control IgG isotype used *in vivo* was purchased from BioXCell (West Lebanon, NH, USA). For *in vitro* cell radiation experiments, cells were seeded in 6-well plates and received fractionated RT at different doses (0 Gy, 8 Gy \times 2, 15 Gy \times 2, 25 Gy \times 2, once a day). The cells were subcultured for 24 h after delivery of fractionated RT and then harvested for analysis.

Tumor cell challenge and treatment

C57BL/6 mice were inoculated subcutaneously (s.c.) with 2×10^5 EL4 cells in both flanks on day 0; the right flank was irradiated at the primary tumor, and the left flank was subjected to out-of-field irradiation of the tumor. Animals were randomly assigned to treatment groups and were subjected to therapies when the tumor volume reached approximately 300 mm³. Irradiation was performed using an RS-2000 irradiator (Rad Source Technologies, Buford, GA, USA). Two fractions of 8 Gy were delivered to a single tumor, whereas for the contralateral tumor, fractionated RT was delivered outside the RT field. Anesthetized mice were positioned in a specific column for fixation, which allowed the area of the primary tumor to be irradiated and protected the rest of the body via a custom 1-cm lead shield. Fractionated RT was applied every other day. α PD-1 mAb and control IgG isotype was administered intraperitoneally at a dose of 200 μ g/mouse (10 mg/kg) every 3 days for a total of three times, starting on day 1 of the fractionated RT cycle (unless otherwise stated). Tumor volume, which was measured using a caliper, was evaluated every 2 days. For tumor rechallenging experiments, LTS mice were implanted with tumor cells at a position remote to the original tumor a minimum of 60 days after previous tumor implantation. Experimental groups that contain at least five mice are representative of at least three independent experiments.

Immunohistochemistry (IHC)

Irradiated cells were embedded in low-melting agarose followed by dehydration and paraffin embedding. Tumors from treated mice were collected, fixed in 4% formalin for 24 h at 4°C, immersed in 75% alcohol, and embedded in paraffin. Primary antibodies used for IHC were as follows: anti-PD-L1 (clone EPR20529; Abcam, Cambridge, UK), anti-PD-1 (clone EPR20665; Abcam), anti-forkhead box P3 (FOXP3; clone 236A/E7; Abcam), anti-CD4 (clone EPR19514; Abcam), anti-CD3 (ab5690; Abcam), and anti-CD8 (ab203035; Abcam), anti-Arginase (ab91279; Abcam), anti-iNOS (ab15323; Abcam), anti-NK1.1 (MA1-70100; Thermo Fisher), anti-MHC I (ER-HR52; Abcam), anti-MHC II (ab25333; Abcam), rabbit anti-mouse (550338; BD), rat anti-mouse (ab6733; Abcam), and mouse anti-mouse (553441; BD). IHC was carried out using an Elivision

Super HRP (Mouse/Rabbit) IHC Kit (KIT-9922, Maixin Biotech) and a Catalyzed Signal Amplification System (K1500, Dako) according to the manufacturer's instructions. Three pathologists analyzed each tissue section. The percentages of positive cells in each visual field were assessed in high-power fields (magnification: 100 \times). Results were averaged and used for statistical analysis. The DLN and spleen were immunostained as positive controls (Supplementary Figure 2(c)).

Flow-cytometric analysis

The blood, spleen, and DLN were harvested on day 7 after treatment. Single-cell suspensions were prepared, and red blood cells were lysed using ACK Lysis Buffer. Antibodies targeting CD4 (GK1.5), CD8 (53-6.7), CD3 (145-2C11), Gr1 (RB6-8C5), CD11b (M1/70), CD45 (30-F11), CD62L (MEL-14), CD44 (IM7), PD-L1 (MIH5), and CD16/CD32 were purchased from eBioscience (Waltham, MA, USA). Antibodies targeting F4/80 (BM8), CD11c (N418), and Ki-67(SOIA15) were purchased from Biolegend (San Diego, CA, USA). Intracellular staining was performed using a fixation/permeabilization kit (eBioscience). The following gating strategies were used for flow cytometry: percentages of CD4⁺ and CD8⁺ after gating on live CD45⁺ CD3⁺ cells. The granulocytic MDSC population is CD11b⁺ and Gr1⁺. The Gr1⁻ portion of the CD11b⁺ population was further subdivided by F4/80 staining. Gr1⁻ CD11b⁺ F4/80⁺ cells are macrophages. The DC population is CD11c⁺. Flow-cytometric analysis was performed using a FACSVerser (Becton Dickinson), and data were analyzed using FlowJo software.

Measurement of interferon (ifn)- γ and interleukin (IL)-2

Serum was collected from treated or control mice. IFN- γ and IL-2 levels were measured using enzyme-linked immunosorbent assay (ELISA) kits (R&D Systems, Minneapolis, MN, USA) according to the manufacturer's instructions. All samples were analyzed in duplicate. The sensitivity of detection was 3 pg/mL. Absorbance was measured at 450 nm. The measured concentration in each sample was normalized to the number of cells counted at the time of harvesting.

Assay of CTL activity in lymphoma-bearing mice

The cytotoxic activity of CTLs was analyzed by MTT assays, as previously described.³³ Briefly, EL4 cells were applied as target cells (T) and were seeded in 96-well U-bottom microtiter plates at 1×10^4 cells/well in 1640 complete medium. Splenocytes were used as effector cells (E). The ratios of effector cells to target cells were 10:1, 20:1, and 40:1. The plates were then incubated for 20 h at 37°C. Twenty microliters of MTT solution (5 mg/mL) was added to each well, and the plates were incubated for another 4 h. To determine the percentage of killed target cells, the following equation was used: CTL activity (%) = $[\text{OD}_T - (\text{OD}_S - \text{OD}_E)] / \text{OD}_T \times 100\%$, where OD_T is the optical density value of the target cell control, OD_E is the optical density value of the effector cell control, and OD_S is the optical density value of samples.

Statistical analysis

Results were expressed as means \pm standard deviations (SDs). All statistical analyses were performed using GraphPad Prism 5 (GraphPad Software, La Jolla, CA, USA) and Origin 6 (OriginLab, Northampton, MA, USA). Student's *t*-tests were used to compare differences between two groups, and one-way analysis of variance was used to compare three or more groups. For survival analysis, Kaplan–Meier curves were analyzed based on log-rank (Mantel–Cox) tests for comparisons of all groups. Differences with *P*-values of 0.05 or less were considered significant.

Abbreviations

PD-1	programmed death-1
PD-L1	programmed death ligand-1
TME	tumor microenvironment
TILs	tumor-infiltrating lymphocytes
RT	radiotherapy
ICD	immunogenic cell death
DAMP	damage-associated molecular pattern
CTL	cytotoxic T lymphocyte
mAb	monoclonal antibody
IgG	immunoglobulin G
LTS	Long-term surviving
IHC	immunohistochemistry
Treg	T regulatory cell
MDSCs	myeloid-derived suppressor cells
DCs	dendritic cell
DLN	draining lymph node

Acknowledgments

We are particularly grateful to Dr. Lieping Chen (Yale University, New Haven, CT USA) and Liqun Luo (Fujian Medical University, Fuzhou, China) for their gift of α PD-1 mAb.

Disclosure of Potential Conflicts of Interest

No potential conflicts of interest were disclosed.

Funding

This study was supported by the Foundation of National science and technology project record (Grant 2016L301); the Foundation of Colleges and universities industry-academic cooperation projects of Fujian Province (Grant 2017Y41010050); the Foundation of Science and technology platform construction project of Fujian Province (Grants 2015Y2102 and 2014Y2101); The Foundation of national science and technology project record [Grant 2016L301]; The Foundation of science and technology platform construction project of Fujian province [Grants 2015Y2102 and 2014Y2101]; The Foundation of colleges and universities industry-academic cooperation project of Fujian province [Grant 2017Y41010050].

References

- Orth M, Lauber K, Niyazi M, Friedl AA, Li M, Maihofer C, Schuttrumpf L, Ernst A, Niemoller OM, Belka C. Current concepts in clinical radiation oncology. *Radiat Environ Biophys.* 2014;53:1–29. PMID:24141602. doi:10.1007/s00411-013-0497-2.
- Vanpouille-Box C, Formenti S, Demaria S. Toward precision radiotherapy for use with immune checkpoint blockers. *Clin Cancer Res.* 2018;24:259–265. PMID:28751442. doi:10.1158/1078-0432.CCR-16-0037.
- Formenti S. Optimizing dose per fraction: A new chapter in the story of the abscopal effect? *Int J Radiat Oncol Biol Phys.* 2017;99:677–679. PMID:29280462. doi:10.1016/j.ijrobp.2017.07.028.
- Valenzuela MT, Nunez MI, Guerrero MR, Villalobos M, Ruiz de Almodovar JM. Capillary electrophoresis of DNA damage after irradiation: apoptosis and necrosis. *J Chromatogr Ar.* 2000;871:321–330. PMID:10735312. doi:10.1016/S0021-9673(99)01245-5.
- Krysko DV, Garg AD, Kaczmarek A, Krysko O, Agostinis P, Vandenabeele P. Immunogenic cell death and DAMPs in cancer therapy. *Nat Rev Cancer.* 2012;12:860–875. PMID:23151605. doi:10.1038/nrc3380.
- Apetoh L, Ghiringhelli F, Tesniere A, Criollo A, Ortiz C, Lidereau R, Mariette C, Chaput N, Mira J, Delaloge S, et al. The interaction between HMGB1 and TLR4 dictates the outcome of anticancer chemotherapy and radiotherapy. *Immunol Rev.* 2007;220:47–59. PMID:17979839. doi:10.1111/j.1600-065X.2007.00573.x.
- Frey B, Ruckert M, Deloch L, Ruhle PF, Derer A, Fietkau R, Gaipl US. Immunomodulation by ionizing radiation-impact for design of radio-immunotherapies and for treatment of inflammatory diseases. *Immunol Rev.* 2017;280:231–248. PMID:29027224. doi:10.1111/imr.12572.
- Medler T, Cotechini T, Coussens L. Immune response to cancer therapy: mounting an effective antitumor response and mechanisms of resistance. *Trends Cancer.* 2015;1:66–75. PMID:26457331. doi:10.1016/j.trecan.2015.07.008.
- Ritprajak P, Azuma M. Intrinsic and extrinsic control of expression of the immunoregulatory molecule PD-L1 in epithelial cells and squamous cell carcinoma. *Oral Oncol.* 2015;51:221–228. PMID:25500094. doi:10.1016/j.oraloncology.2014.11.014.
- Zou W, Wolchok JD, Chen L. PD-L1 (B7-H1) and PD-1 pathway blockade for cancer therapy: mechanisms, response biomarkers, and combinations. *Sci Transl Med.* 2016;8:328rv324. PMID:26936508. doi:10.1126/scitranslmed.aad71118.
- Zou W, Chen L. Inhibitory B7-family molecules in the tumour microenvironment. *Nat Rev Immunol.* 2008;8:467–477. PMID:18500231. doi:10.1038/nri2326.
- Taube J, Anders R, Young G, Xu H, Sharma R, McMiller T, Chen S, Klein A, Pardoll D, Topalian S, et al. Colocalization of inflammatory response with B7-h1 expression in human melanocytic lesions supports an adaptive resistance mechanism of immune escape. *Sci Transl Med.* 2012;4:127ra137. PMID:22461641. doi:10.1126/scitranslmed.3003689.
- Wolchok JD, Kluger H, Callahan MK, Postow MA, Rizvi NA, Lesokhin AM, Segal NH, Ariyan CE, Gordon RA, Reed K, et al. Nivolumab plus ipilimumab in advanced melanoma. *N Engl J Med.* 2013;369:122–133. PMID:23724867. doi:10.1056/NEJMoa1302369.
- Tumeh PC, Harview CL, Yearley JH, Shintaku IP, Taylor EJM, Robert L, Chmielowski B, Spasic M, Henry G, Ciobanu V, et al. PD-1 blockade induces responses by inhibiting adaptive immune resistance. *Nature.* 2014;515:568–571. PMID:25428505. doi:10.1038/nature13954.
- Topalian SL, Hodi FS, Brahmer JR, Gettinger SN, Smith DC, McDermott DF, Powderly JD, Carvajal RD, Sosman JA, Atkins MB, et al. Safety, activity, and immune correlates of anti-PD-1 antibody in cancer. *N Engl J Med.* 2012;366:2443–2454. PMID:22658127. doi:10.1056/NEJMoa1200690.
- Sakuishi K, Apetoh L, Sullivan JM, Blazar BR, Kuchroo VK, Anderson AC. Targeting Tim-3 and PD-1 pathways to reverse T cell exhaustion and restore anti-tumor immunity. *J Exp Med.* 2010;207:2187–2194. PMID:20819927. doi:10.1084/jem.20100643.
- Ribas A. 2012. Tumor immunotherapy directed at PD-1. *N Engl J Med.* 366:2517–2519. doi:10.1056/NEJMe1205943.
- Lipson EJ, Sharfman WH, Drake CG, Wollner I, Taube JM, Anders RA, Xu H, Yao S, Pons A, Chen L, et al. Durable cancer regression off-treatment and effective reinduction therapy with an anti-PD-1 antibody. *Clin Cancer Res.* 2013;19:462–468. PMID:23169436. doi:10.1158/1078-0432.CCR-12-2625.

19. Powles T, Eder JP, Fine GD, Braiteh FS, Loria Y, Cruz C, Bellmunt J, Burris HA, Petrylak DP, Teng SL, et al. MPDL3280A (anti-PD-L1) treatment leads to clinical activity in metastatic bladder cancer. *Nature*. 2014;515:558–562. PMID:25428503. doi:10.1038/nature13904. doi:10.1038/nature13904.
20. Brahmer J, Reckamp K, Baas P, Crinò L, Eberhardt W, Poddubskaya E, Antonia S, Pluzanski A, Vokes E, Holgado E, et al. Nivolumab versus docetaxel in advanced squamous-cell non-small-cell lung cancer. *N Engl J Med*. 2015;373:123–135. PMID: 26028407. doi:10.1056/NEJMoa1504627.
21. Motzer RJ, Escudier B, McDermott DF, George S, Hammers HJ, Srinivas S, Tykodi SS, Sosman JA, Procopio G, Plimack ER, et al. Nivolumab versus Everolimus in Advanced Renal-Cell Carcinoma. *N Engl J Med*. 2015;373:1803–1813. PMID:26406148. doi:10.1056/NEJMoa1510665.
22. Siva S, MacManus MP, Martin RF, Oa M. Abscopal effects of radiation therapy: a clinical review for the radiobiologist. *Cancer Lett*. 2015;356:82–90. PMID:24125863. doi:10.1016/j.canlet.2013.09.018.
23. Brix N, Tiefenthaler A, Anders H, Belka C, Lauber K. Abscopal, immunological effects of radiotherapy: narrowing the gap between clinical and preclinical experiences. *Immunol Rev*. 2017;280:249–279. PMID: 29027221. doi:10.1111/imr.12573.
24. Mole R. Whole body irradiation; radiobiology or medicine? *Br J Radiol*. 1953;26:234–241. doi:10.1259/0007-1285-26-305-234.
25. Derer A, Spiljar M, Bäuml M, Hecht M, Fietkau R, Frey B, Gaipl U. Chemoradiation Increases PD-L1 expression in certain melanoma and glioblastoma cells. *Front Immunol*. 2016;7:610. PMID: 28066420. doi:10.3389/fimmu.2016.00610.
26. Kikuchi M, Clump D, Srivastava R, Sun L, Zeng D, Diaz-Perez J, Anderson C, Edwards W, Ferris R. Preclinical immunoPET/CT imaging using Zr-89-labeled anti-PD-L1 monoclonal antibody for assessing radiation-induced PD-L1 upregulation in head and neck cancer and melanoma. *Oncoimmunology*. 2017;6:7. PMID: 28811971. doi:10.1080/2162402X.2017.1329071.
27. Weichselbaum R, Liang H, Deng L, Fu Y. Radiotherapy and immunotherapy: a beneficial liaison? *Nat Rev Clin Oncol*. 2017;14:365–379. PMID: 28094262. doi:10.1038/nrclinonc.2016.211.
28. Ngwa W, Irabor O, Schoenfeld J, Hesser J, Demaria S, Formenti S. Using immunotherapy to boost the abscopal effect. *Nat Rev Cancerr*. 2018;18:313–322. PMID: 29449659. doi:10.1038/nrc.2018.6.
29. Wang M, Wang H, Tang Y, Kang D, Gao Y, Ke M, Dou J, Xi T, Zhou C. Effective inhibition of a *Strongylocentrotus nudus* eggs polysaccharide against hepatocellular carcinoma is mediated via immunoregulation in vivo. *Immunol Lett*. 2011;141:74–82. PMID: 21893096. doi:10.1016/j.imlet.2011.08.001.
30. Duraiswamy J, Kaluza KM, Freeman GJ, Coukos G. Dual blockade of PD-1 and CTLA-4 combined with tumor vaccine effectively restores T-cell rejection function in tumors. *Cancer Res*. 2013;73:3591–3603. PMID:23633484. doi:10.1158/0008-5472.CAN-12-4100.
31. Dovedi S, Adlard A, Lipowska-Bhalla G, McKenna C, Jones S, Cheadle E, Stratford I, Poon E, Morrow M, Stewart R, et al. Acquired resistance to fractionated radiotherapy can be overcome by concurrent PD-L1 blockade. *Cancer Res*. 2014;74:5458–5468. PMID: 25274032. doi:10.1158/0008-5472.CAN-14-1258.
32. Wilcox RA, Flies DB, Zhu G, Johnson AJ, Tamada K, Chapoval AI, Strome SE, Pease LR, Chen L. Provision of antigen and CD137 signaling breaks immunological ignorance, promoting regression of poorly immunogenic tumors. *J Clin Invest*. 2002;109:651–659. PMID:11877473. doi:10.1172/JCI14184.
33. Xu HS, Wu YW, Xu SF, Sun HX, Chen FY, Yao L. Antitumor and immunomodulatory activity of polysaccharides from the roots of *Actinidia eriantha*. *J Ethnopharmacol*. 2009;125:310–317. PMID:19559777. doi:10.1016/j.jep.2009.06.015.